Journal of Applied Physics ARTICLE scitation.org/journal/jap

Radiation defect dynamics in SiC with pre-existing defects

Cite as: J. Appl. Phys. **125**, 235706 (2019); doi: 10.1063/1.5093640
Submitted: 22 February 2019 · Accepted: 1 June 2019 ·
Published Online: 18 June 2019

L. B. Bayu Aji,[a] J. B. Wallace, and S. O. Kucheyev

AFFILIATIONS

Lawrence Livermore National Laboratory, Livermore, California 94550, USA

[a]**Electronic mail:** bayuaji1@llnl.gov

ABSTRACT

The influence of pre-existing lattice disorder on radiation defect dynamics in SiC remains unexplored. Here, we use a pulsed ion beam method to study dynamic annealing in Ar-ion-bombarded 3*C*-SiC at 200 °C with different levels of pre-existing lattice disorder. Results reveal a nonmonotonic dependence of the defect relaxation time constant on the level of pre-existing disorder, exhibiting a maximum of ∼4 ms at a level of relative initial disorder of ∼0.4, while crystals without pre-existing damage are characterized by a time constant of ∼1.4 ms. These observations demonstrate that radiation defect dynamics in SiC can be controlled by defect engineering.

I. INTRODUCTION

Due to a combination of its unique properties, 3*C*-SiC is an attractive material for several applications in electronics and nuclear engineering.[1,2] The understanding of radiation damage processes in 3*C*-SiC is directly relevant to both electronics and nuclear technologies. The formation of radiation damage in SiC is a complex, multistage phenomenon.[2–13] It intricately depends on irradiation conditions, such as ion mass, energy, dose, dose rate, and target temperature (T). It is also influenced by the presence of stable defects that could interact with ion-beam-generated mobile point defects during ion irradiation via so-called dynamic annealing (DA). Pre-existing disorder can either enhance or suppress the efficiency of the formation of stable defects and could change rates of the dominant defect interaction processes. Such an influence of stable lattice defects on radiation damage formation in 3*C*-SiC remains essentially unexplored.

Here, we report how pre-existing stable defects influence DA in 3*C*-SiC bombarded at 200 °C with 500 keV Ar ions. To access the DA regime, we use a pulsed ion beam method[15,14,16,13] when the total ion dose is delivered as a train of equal square pulses, each with a duration of t_{on} and an instantaneous dose rate of F_{on}, separated by a passive portion of the beam duty cycle of t_{off} (see the inset in Fig. 1). Our results reveal a nonmonotonic dependence of the DA rate on the level of pre-existing disorder, clearly demonstrating that defect interaction dynamics in 3*C*-SiC can be controlled by defect engineering.

II. EXPERIMENT

We used single-crystal epilayers of (001) 3*C*-SiC (on Si wafers with a diameter of 100 mm) obtained from NOVASiC. The epilayers had a thickness of $\gtrsim 2\,\mu$m and a resistivity of 1–10 Ω cm. Samples were bombarded at (200 ± 1) °C with 500 keV Ar ions at ∼7° off the [100] direction to minimize channeling. All irradiation experiments described here (with either continuous or pulsed beams) were performed in a broad beam mode rather than with rastered beams.[15] Samples with pre-existing defects were prepared by irradiation of as-grown epilayers at 200 °C with a continuous 500 keV Ar ion beam with a dose rate of 1.9×10^{14} cm^{-2} s^{-1} to doses ranging from 0.15 to 0.82 displacements per atom (DPA).

Radiation defect dynamics in samples with and without such pre-existing defects was measured by the pulsed beam method[15,14,16,13] at 200 °C with 500 keV Ar ions with $t_{on} = 1$ ms, $F_{on} = 1.9 \times 10^{13}$ cm^{-2} s^{-1}, and t_{off} varied between 1 and 50 ms. A more detailed description of the experimental arrangement can be found elsewhere.[15,16]

The dependence of lattice damage in the Si sublattice on t_{off} was studied *ex situ* at room temperature by ion channeling with 2 MeV ^{4}He$^+$ ions incident along the [100] direction and backscattered into a detector at 164° relative to the incident beam direction. Channeling spectra were analyzed with one of the conventional algorithms[17] for extracting depth profiles of relative disorder. Values of average bulk relative disorder (n, with $n = 1$ corresponding to amorphization) were obtained by averaging over 15 channels

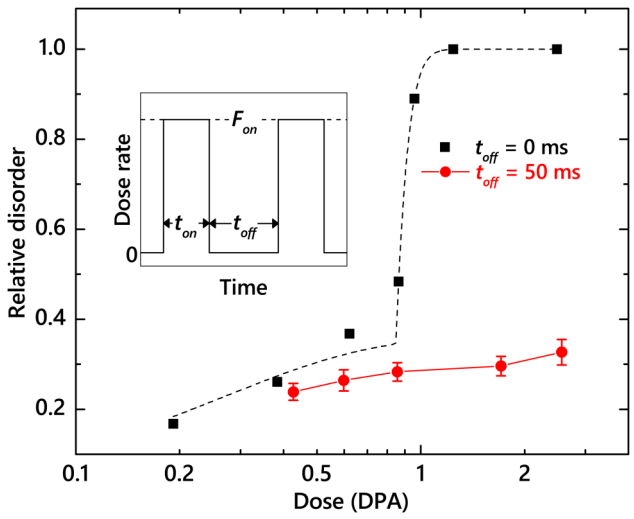

FIG. 1. Dose dependencies of the maximum level of relative disorder in the crystal bulk for 3*C*-SiC bombarded at 200 °C with 500 keV Ar ions with a continuous beam (i.e., $t_{off} = 0$ ms) with a dose rate of 1.9×10^{13} cm^{-2} s^{-1} (from Ref. 11) and with a pulsed beam with $F_{on} = 1.9 \times 10^{13}$ cm^{-2} s^{-1}, $t_{on} = 1$ ms, and $t_{off} = 50$ ms. The dashed line depicts the result of fitting with a stimulated amorphization model from Ref. 11. The inset shows a schematic of the time dependence of the dose rate in pulsed beam experiments, defining t_{on}, t_{off}, and F_{on}.

(~40 nm) centered on the bulk defect peak. Error bars of n are standard deviations.

The depth profile of ballistically generated vacancies was calculated with the TRIM code (version SRIM-2013.00, full cascade calculations)[18] with an atomic concentration of SiC of 9.64×10^{22} atoms cm^{-3} (Ref. 2) and threshold energies for atomic displacements of 20 and 35 eV for C and Si sublattices, respectively.[19] The projected range and straggle of 500 keV Ar ions are 320 and 70 nm, respectively. To convert to DPAs (at the depth corresponding to the maximum of the vacancy generation profile), ion doses in 10^{16} Ar ions cm^{-2} are multiplied by 8.98.

III. RESULTS AND DISCUSSION

As described previously,[15,14,16,13] pulsed beam experiments start with the measurement of traditional damage buildup curves to define the ion dose of interest. Figure 1 compares dose dependencies of the bulk disorder level for continuous ($t_{off} = 0$ ms) and pulsed ($t_{on} = 1$ ms, $t_{off} = 50$ ms) beams of 500 keV Ar ions. Such a pulsed beam irradiation with a small $\frac{t_{on}}{t_{off}}$ ratio approaches the condition of very low dose rates when the interaction of mobile defects generated in different collision cascades is minimized. The sigmoidal shape of damage buildup curves is consistent with several previous reports.[4,5,10] Also shown in Fig. 1 by the dashed line is fitting with a phenomenological stimulated amorphization model from Ref. 11. Such fitting gives the following parameters: $f^{sat}_{cluster} = 0.36$ (the maximum saturation fraction of defect clusters in the lattice), $\Phi_{crit} = 0.85 \pm 0.01$ DPA (the critical dose above which amorphization proceeds), $\Phi_{amorph} = 1.03 \pm 0.02$ DPA (the amorphization dose), $\sigma_{cluster} = 3.73 \pm 0.46$ DPA s^{-1} (the cluster production cross section), and $\xi_{amorph} = 17.6 \pm 2.6$ DPA^{-2} (the amorphization cross-section constant). Figure 1 clearly shows that, in the entire dose range studied, damage buildup depends on the effective dose rate. The dose-rate dependence is particularly pronounced for doses above ~1 DPA when a rapid super-linear increase in the damage level is observed for continuous but not for pulsed-beam bombardment. This behavior reflects strong DA in 3*C*-SiC at 200 °C.[11,12] Based on the damage buildup data from Fig. 1, we have chosen doses for pulsed beam experiments so that, for continuous beam irradiation, n was ~0.6 for samples with different levels of pre-existing disorder.

Figure 2 shows representative depth profiles of relative disorder for bombardment with continuous ($t_{off} = 0$ ms) and pulsed ($t_{off} = 5$ and 30 ms) ion beams for samples without pre-existing disorder [Fig. 2(a)] and samples with three different levels of pre-existing disorder [Figs. 2(b)–2(d)]. Each panel in Fig. 2 shows data for cases when all the irradiation conditions, except for t_{off}, were kept constant. All these profiles are bimodal, with the first small peak at the sample surface and the second major peak (whose maximum we refer to as n) in the crystal bulk. The bulk peak is centered on ~320 nm, corresponding to the maximum of the depth profile of vacancies ballistically generated by 500 keV Ar ion bombardment.[18]

It is also seen from Fig. 2 that n decreases with increasing t_{off}, while the damage level at the surface remains unchanged, suggesting different mechanisms of bulk and surface disordering. These observations are consistent with results of previous pulsed beam and dose-rate studies of Si and SiC.[15,20–22,12,23] We have found such a reduction in n with increasing t_{off} in all the measurements for samples with different levels of pre-existing disorder ($n_{initial}$). This is illustrated in Fig. 2 and summarized in Fig. 3(a). Solid lines in Fig. 3(a) are fits of the data via the Marquardt-Levenberg algorithm with the second order decay equation: $n(t_{off}) = n_\infty + \frac{n(0)-n_\infty}{1+\frac{t_{off}}{\tau}}$. Here, n_∞ is the relative disorder for $t_{off} \gg \tau$. All the $n(t_{off})$ dependencies from Fig. 3 obey the second order decay (with a coefficient of determination of > 0.98) better than the first order (i.e., exponential) decay.

The effect of pre-existing damage on τ is summarized in Fig. 4 (left axis), revealing a nonmonotonic $\tau(n_{initial})$ behavior, with a maximum at $n_{initial} \approx 0.4$. Such a $\tau(n_{initial})$ dependence could be related not only to the interaction of radiation-generated point defects with pre-existing disorder but also to the fact that these pulsed beam experiments [i.e., measurements of $n(t_{off})$ dependencies] with different $n_{initial}$ levels span different ranges of disorder. Indeed, the $n(t_{off})$ dependencies shown in Fig. 3(a) were measured with different pulsed beam doses. For example, samples with $n_{initial} = 0.18$ received an ~1.2 times larger pulsed beam irradiation doses than for the case of $n_{initial} = 0.28$. Hence, in order to differentiate between effects of pre-existing disorder and a possible influence of different damage levels probed in these experiments, we have measured $n(t_{off})$ dependencies for a series of samples without any pre-existing disorder (i.e., $n_{initial} = 0$) but with different doses.

Plotted in Fig. 3(b) is the $n(t_{off})$ dependence for doses ranging from 0.45 to 0.94 DPA. Solid lines are fits of the data via the

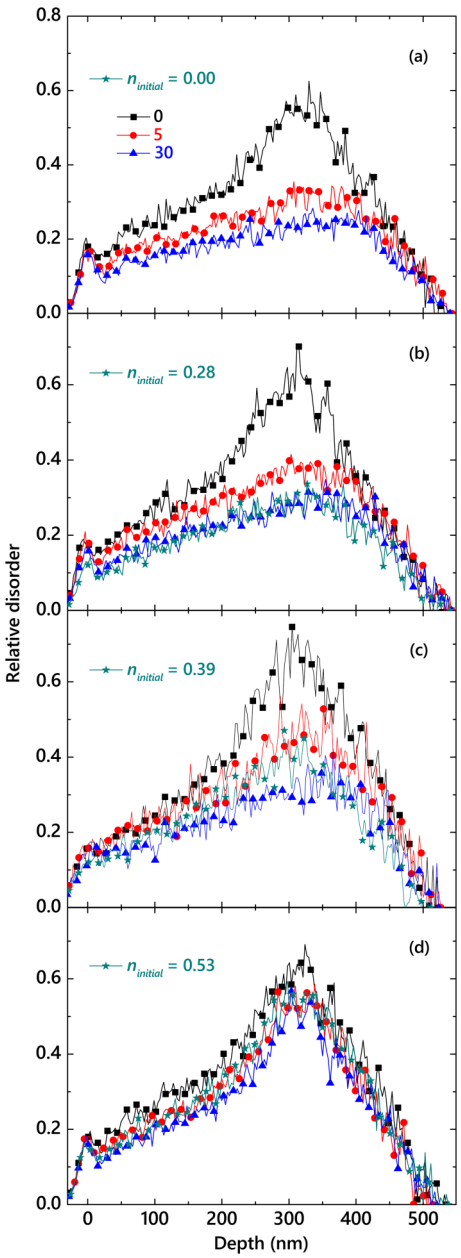

FIG. 2. Selected depth profiles of relative disorder for irradiation at 200 °C of (a) pristine 3C-SiC and samples with maximum levels of pre-existing bulk disorder ($n_{initial}$) of (b) 0.28, (c) 0.39, and (d) 0.53. Pulsed beam irradiation was done with 500 keV Ar ions with $F_{on} = 1.9 \times 10^{13}$ cm^{-2} s^{-1}, $t_{on} = 1$ ms, doses of (a) 0.88, (b) 0.43, (c) 0.26, and (d) 0.06 DPA, and with different t_{off} values, given in legend in (a) in milliseconds, which applies to all four panels. Pre-existing disorder shown by star symbols in (b), (c), and (d) was produced by irradiation at 200 °C with a continuous beam of 500 keV Ar ions with a dose rate of 1.9×10^{14} cm^{-2} s^{-1} to doses of 0.45, 0.62, and 0.82 DPA, respectively, so that the total dose (i.e., the combined dose of continuous and pulsed beam irradiation) was 0.88 DPA, the same for all the cases. For clarity, only every 10th experimental point is depicted in all the profiles.

Marquardt-Levenberg algorithm with the second order decay equation. Fitting results are summarized in Fig. 5 (left axis), showing that, for samples with $n_{initial} = 0$, τ is ~1.4 ms, within experimental errors independent of the dose used. The $\tau(n_{initial})$ dependence from Fig. 4 (left axis) is, therefore, attributed to the interaction of radiation-generated point defects with pre-existing disorder. It is also seen from Fig. 3(b) that, for large t_{off}, the damage level saturates at ~0.25 and is essentially independent of the dose used. This is consistent with Fig. 1, revealing that the damage level saturates with dose for irradiation with large t_{off}, which is similar to a condition of very low dose rates when the

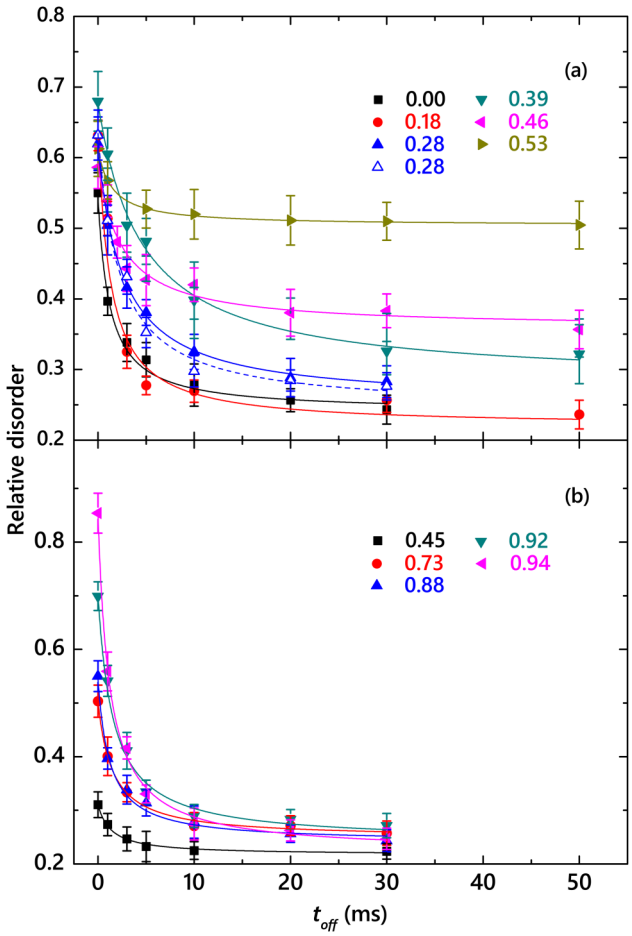

FIG. 3. Average bulk relative disorder in 3C-SiC bombarded at 200 °C with pulsed beams of 500 keV Ar ions with $F_{on} = 1.9 \times 10^{13}$ cm^{-2} s^{-1} and $t_{on} = 1$ ms as a function of the passive portion of the beam duty cycle (t_{off}) for (a) samples with different levels of pre-existing disorder ($n_{initial}$, given in the legend) created by continuous beam irradiation and (b) samples without pre-existing disorder but irradiated to different pulsed-beam doses (given in the legend in units of DPA). The total dose for all data shown in (a) was 0.88 DPA. Open symbols in (a) show data points for samples with $n_{initial} = 0.28$ produced by pulsed beam irradiation with $F_{on} = 1.9 \times 10^{13}$ cm^{-2} s^{-1}, $t_{on} = 1$ ms, and $t_{off} = 50$ ms. Fitting curves with the second order decay equation are shown by lines.

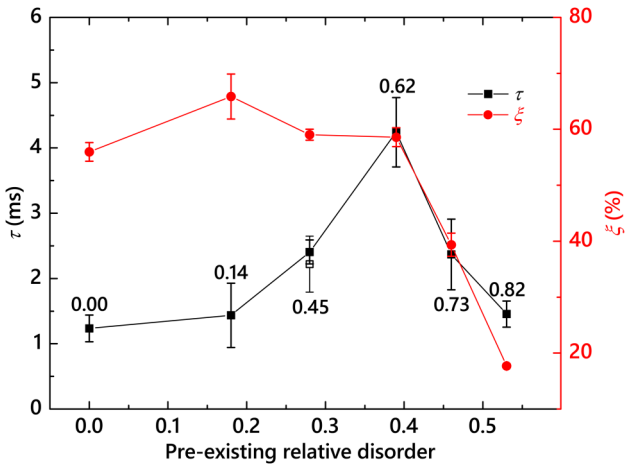

FIG. 4. (Closed symbols) Dependencies of (left axis) the defect relaxation time constant (τ) and (right axis) the dynamic annealing efficiency (ξ) on the level of average bulk relative disorder present in samples before pulsed ion beam irradiation. Open symbols show data points for samples with pre-existing disorder produced by pulsed beam irradiation with $F_{on} = 1.9 \times 10^{13}$ cm^{-2} s^{-1}, $t_{on} = 1$ ms, and $t_{off} = 50$ ms. Numbers next to data points indicate ion doses (in units of DPA) of continuous beam irradiation used to create such pre-existing disorder.

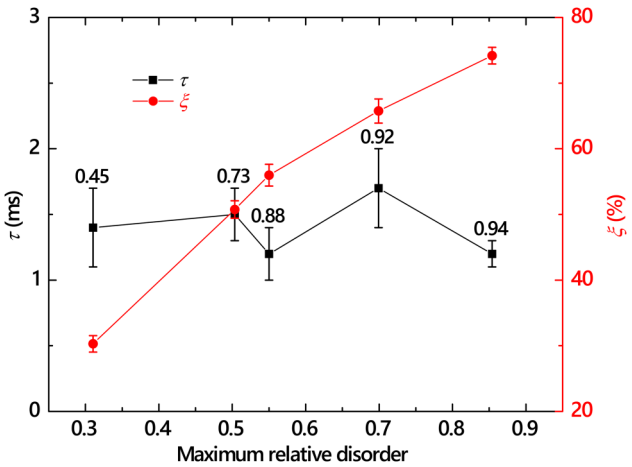

FIG. 5. Dependencies of (left axis) the defect relaxation time constant (τ) and (right axis) the dynamic annealing efficiency (ξ) on the maximum average bulk relative disorder level for samples without pre-existing defects. Numbers next to data points indicate the total pulsed Ar ion doses used (in units of DPA).

interaction of mobile defects generated in different collision cascades is minimized. The existence of such a damage saturation regime could be explored in future studies aimed at identifying and designing radiation tolerant materials for irradiation conditions with strong DA and negligible intercascade defect interaction.

The nonmonotonic $\tau(n_{initial})$ dependence of Fig. 4 suggests a change in the dominant mechanism of the interaction of point defects with pre-existing disorder starting at $n_{initial} \approx 0.4$. Interestingly, this disorder level corresponds to $f^{sat}_{cluster}$. As discussed in detail previously,[11,12] in this relatively low dose regime resulting in $n \lesssim 0.4$, stable pre-existing lattice defects are predominantly in the form of point defect clusters that could act as efficient traps for ion-beam-generated mobile point defects. An increase in the concentration of such defect clusters could explain the slowing down of defect relaxation dynamics with increasing $n_{initial}$ as revealed in Fig. 4. Such slowing of the defect relaxation dynamics with increasing level of pre-existing disorder for $n_{initial} \lesssim 0.4$ could be reflecting the trapping of migrating point defects at shallow energy levels associated with point defect clusters, followed by subsequent detrapping. This trapping-detrapping process does not necessarily involve defect recombination but would lead to an increase in τ. The inflection point of the damage buildup curve at $n_{initial} \approx 0.4$ reflects the onset of lattice amorphization.[11,12] Results from Fig. 4, therefore, suggest that the presence of amorphous zones speeds up DA processes, while point defect clusters slow them down. However, more work is currently needed to better understand the mechanisms of point defect trapping at clusters and amorphous zones and their influence on defect relaxation dynamics.

Figure 4 (right axis) plots the DA efficiency (ξ) as a function of $n_{initial}$, while Fig. 5 (right axis) shows the dependence of ξ on the maximum average bulk relative disorder level for samples without pre-existing defects. Here, we define ξ as $(n(0) - n_\infty)/(n(0) - n_{initial})$. As discussed in detail in our previous study,[16] for our choice of F_{on} and t_{on}, ξ is the magnitude of the dose-rate effect; i.e., the difference between stable disorder for irradiation with continuous beams with dose rates of $F = F_{on}$ and $F \to 0$. It is seen that ξ depends strongly on both the total dose in pulsed beam experiments and on $n_{initial}$. However, these two dependencies are qualitatively different, with ξ increasing with the total dose (Fig. 5) and decreasing with $n_{initial}$ for $n_{initial} \gtrsim 0.4$ (Fig. 4). It is also seen from Fig. 4 that ξ is essentially independent of $n_{initial}$ for $n_{initial} < 0.4$. This further supports the above suggestion that trapping-detrapping processes at point defect clusters for damage levels $\lesssim$0.4 do not necessarily involve defect recombination but could significantly slow down defect interaction dynamics manifested as a strong increase in τ. The decrease in ξ with increasing $n_{initial}$ above 0.4 reflects a reduction in the total fraction of mobile point defects participating in DA. In contrast, an increase in ξ with increasing total ion dose in pulsed beam experiments (Fig. 5) indicates that DA in 3*C*-SiC is more pronounced in regimes of larger doses, which is consistent with damage buildup curves from Fig. 1 and our previous systematic studies of the dose-rate effect.[12]

Finally, Fig. 3 includes one data set for the case of $n_{initial} = 0.28$ produced by pulsed-beam irradiation with $\frac{t_{on}}{t_{off}} \ll 1$, approaching the condition of very low dose rate irradiation when the interaction of defects generated in different collision cascades is minimized. It reveals that τ for $n_{initial} = 0.28$ is independent of the dose rate used for creating pre-existing disorder. This finding is in agreement with results of our previous systematic study of the effect of the dose rate on damage accumulation in 3*C*-SiC.[12] It has shown that irradiation with continuous Ar ion beams with a dose rate of 4.2×10^{13} cm^{-2} s^{-1} results in only a slightly (~20%) larger average size of defect clusters than for the case of lower dose-rate irradiation.

IV. CONCLUSIONS

In conclusion, we have studied the defect interaction dynamics in 3C-SiC with pre-existing defects bombarded at 200 °C with 500 keV Ar ions. The defect relaxation time constant strongly and nonmonotonically depends on the level of pre-existing disorder. These observations clearly demonstrate that defect engineering can be used to control DA in SiC and reveal additional complexity of defect interaction processes with important implications for benchmarking future work on theory and modeling of radiation damage in this material.

ACKNOWLEDGMENTS

This work was performed under the auspices of the U.S. DOE by LLNL under Contract No. DE-AC52-07NA27344. J.B.W. acknowledges the LGSP for funding.

REFERENCES

[1]A. Fissel, "Artificially layered heteropolytypic structures based on SiC polytypes: Molecular beam epitaxy, characterization and properties," Phys. Rep. **379**, 149–255 (2003).
[2]L. L. Snead, T. Nozawa, Y. Katoh, T. S. Byun, S. Kondo, and D. A. Petti, "Handbook of SiC properties for fuel performance modeling," J. Nucl. Mater. **371**, 329–377 (2007).
[3]H. Inui, H. Mori, A. Suzuki, and H. Fujita, "Electron-irradiation-induced crystalline-to-amorphous transition in β-SiC single crystals," Philos. Mag. B **65**, 1–14 (1992).
[4]W. J. Weber, and L. M. Wang, "The temperature dependence of ion-beam-induced amorphization in β-SiC," Nucl. Instrum. Methods B **106**, 298–302 (1995).
[5]L. L. Snead, S. J. Zinkle, J. C. Hay, and M. C. Osborne, "Amorphization of SiC under ion and neutron irradiation," Nucl. Instrum. Methods B **141**, 123–132 (1998).
[6]W. J. Weber, N. Yu, and L. M. Wang, "Irradiation-induced amorphization in β-SiC," J. Nucl. Mater. **253**, 53–59 (1998).
[7]A. Yu. Kuznetsov, J. Wong-Leung, A. Hallén, C. Jagadish, and B. G. Svensson, "Dynamic annealing in ion implanted SiC: Flux versus temperature dependence," J. Appl. Phys. **94**, 7112–7115 (2003).
[8]Y. Zhang, W. J. Weber, W. Jiang, C. M. Wang, V. Shutthanandan, and A. Hallén, "Effects of implantation temperature on damage accumulation in Al-implanted 4H-SiC," J. Appl. Phys. **95**, 4012–4018 (2004).
[9]E. Wendler, T. Bierschenk, W. Wesch, E. Friedland, and J. B. Malherbe, "Temperature dependence of damage formation in Ag ion irradiated 4H-SiC," Nucl. Instrum. Methods B **268**, 2996–3000 (2010).
[10]A. Debelle, L. Thome, D. Dompoint, A. Boulle, F. Garrido, J. Jagielski, and D. Chaussende, "Characterization and modelling of the ion-irradiation induced disorder in 6H-SiC and 3C-SiC single crystals," J. Phys. D Appl. Phys. **43**, 455408 (2010).
[11]J. B. Wallace, L. B. Bayu Aji, T. T. Li, L. Shao, and S. O. Kucheyev, "Damage buildup in Ar-ion-irradiated 3C-SiC at elevated temperatures," J. Appl. Phys. **118**, 105705 (2015).
[12]L. B. Bayu Aji, T. T. Li, J. B. Wallace, and S. O. Kucheyev, "Dose-rate dependence of damage buildup in 3C-SiC," J. Appl. Phys. **121**, 235106 (2017).
[13]J. B. Wallace, L. B. Bayu Aji, L. Shao, and S. O. Kucheyev, "Radiation defect dynamics studied by pulsed ion beams" Nucl. Instrum. Methods Phys. Res. **409**, 347–350 (2017).
[14]J. B. Wallace, L. B. Bayu Aji, L. Shao, and S. O. Kucheyev, "Time constant of defect relaxation in ion-irradiated 3C-SiC," Appl. Phys. Lett. **106**, 202102 (2015).
[15]M. T. Myers, S. Charnvanichborikarn, L. Shao, and S. O. Kucheyev, "Pulsed ion beam measurement of the time constant of dynamic annealing in Si," Phys. Rev. Lett. **109**, 095502 (2012).
[16]J. B. Wallace, S. Charnvanichborikarn, L. B. Bayu Aji, M. T. Myers, L. Shao, and S. O. Kucheyev, "Radiation defect dynamics in Si at room temperature studied by pulsed ion beams," J. Appl. Phys. **118**, 135709 (2015).
[17]K. Schmid, "Some new aspects for the evaluation of disorder profiles in silicon by backscattering," Radiat. Eff. **17**, 201–207 (1973).
[18]J. F. Ziegler, M. D. Ziegler, and J. P. Biersack, "SRIM—The stopping and range of ions in matter," Nucl. Instrum. Methods B **268**, 1818–1823 (2010).
[19]R. Devanathan, W. J. Weber, and F. Gao, "Atomic scale simulation of defect production in irradiated 3C-SiC," J. Appl. Phys. **90**, 2303–2309 (2001).
[20]J. B. Wallace, L. B. Bayu Aji, L. Shao, and S. O. Kucheyev, "Fractal analysis of collision cascades in pulsed-ion-beam-irradiated solids," Sci. Rep. **7**, 17574 (2017).
[21]L. B. Bayu Aji, J. B. Wallace, and S. O. Kucheyev, "Effects of collision cascade density on radiation defect dynamics in 3C-SiC," Sci. Rep. **7**, 44703 (2017).
[22]L. B. Bayu Aji, J. B. Wallace, and S. O. Kucheyev, "Radiation defect dynamics in 3C-, 4H-, and 6H-SiC studied by pulsed ion beams," Nucl. Instrum. Methods Phys. Res. **435**, 8–11 (2018).
[23]A. I. Titov and G. Carter, "Defect accumulation during room temperature N irradiation of silicon," Nucl. Instrum. Methods Phys. Res. **119**, 491–500 (1996).